Colloid and Interface Science Communications 17 (2017) 10–13

Contents lists available at ScienceDirect

Colloid and Interface Science Communications

journal homepage: www.elsevier.com/locate/colcom

Design Principles for the Formation of Ordered Patterns in Binary Mixtures of Colloidal Particles on Spherical Droplets

Sara Fortuna[a,*], David L. Cheung[b]

[a]Center for Biomedical Sciences and Engineering, University of Nova Gorica, Vipava, Slovenia
[b]School of Chemistry, National University of Ireland Galway, University Road, Galway, Ireland

ARTICLE INFO

Article history:
Received 14 August 2016
Accepted 26 February 2017
Available online 11 March 2017

ABSTRACT

We elucidate the design principles for the formation of ordered structures formed by binary mixtures of particles on spherical surfaces, such as emulsion droplets, polymer vesicles, and colloidal nanoparticles. Using grand-canonical Monte Carlo simulations we explore different potential parameters observing a number of packing patterns. Interparticle interactions are described using a combination of Lennard-Jones and Yukawa potentials, mimicking the short-range attraction, long-range repulsion often observed in colloidal systems. We show that the strength of the electrostatic interaction is one of the key parameters driving the formation of ordered patterns. We also show that the formation of Janus particles, through segregation of different types of particles, is possible for carefully chosen parameter combinations and identify regions of the parameter space presenting each pattern.

The assembly of colloidal particles, both in bulk and on surfaces, is an active area of research [1]. It allows for the creation of materials with novel properties, with applications in areas including photonics [2], catalysis [3], and sensing [4]. Assembly on surfaces is of particular interest, as the surface structure can be used to direct the assembly of colloidal particles [5]. Adsorption of colloids onto spherical droplets or particles allows for the combination of different materials into core-shell architectures with applications in catalysis [6], drug delivery [7], and the design of stimuli-responsive materials [8]. Engineering surfaces by the co-adsorption of surfactants with different chemical properties further allows for the design of hybrid materials capable of performing multiple functions [9]. For instance, polymer vesicles can be armored with amphiphilic molecules, such as poly(ethylenimine) [10], and colloidal nanoparticles such as polystyrene latex spheres, silica nanoparticles, partially film-formed poly(n-butyl methacrylate) latex particles, and a poly((ethyl acrylate)-co-(methacrylic acid)) hydrogel [11,12] and can be synthesized following several routes [13] generally following a bottom-up approach [14].

On curved surfaces perfect hexagonal packing is impossible to achieve, even in the case of perfectly monodisperse particles. In the most ideal case of identical particles on a spherical surface, the hexagonal packing is disrupted by the formation of 12 pentacoordinated defects [15]. Theoretical studies, using molecular dynamics [16] or Monte Carlo (MC) simulations [17], have shown that this ideal case typically only exists when the central sphere is small, compared to the size of the adsorbed particles. When this is not the case line defects or scars are observed [12,18]. When the particles adsorbed on the sphere are composed of a mixture of different sizes the packing is expected to be more complex. The differing particle sizes disrupt the packing, potentially leading to demixing driven purely by the size difference. Introducing size-dependent Lennard-Jones (LJ) and electrostatic interaction between the different types of adsorbed particles can lead to richer phase behaviour.

When the small size of the supporting particle (with respect to the adsorbed particles) prohibits the formation of large scale order [11,12], the interplay between the attractive and repulsive interactions allows for the formation of a range of microphase separated structures. Understanding these structures requires knowledge of the interplay between the different interactions in the system. Molecular simulations have been demonstrated that it is theoretically possible to form striped patterns on spherical particles [19], while Janus particles have been formed through the assembly of incompatible surfactants on nanoparticles [20]. In addition, it has been shown by MC simulations that ordered shells or randomly arranged patterns can be obtained either by charge-dependent repulsive interactions or size-dependent LJ interactions [21]. Furthermore both the surface coverage and patterns

* Corresponding author.
E-mail addresses: sara.fortuna@ung.si (S. Fortuna), david.cheung@nuigalway.ie (D.L. Cheung).
URL: http://www.sarafortuna.eu (S. Fortuna).

http://dx.doi.org/10.1016/j.colcom.2017.02.002

formed are not simply determined by the ratio of particles in solution (or equivalently the chemical potentials) as demonstrated by MC simulations [11].

Despite this previous work, a general understanding of the pattern formation of particles on a spherical surface is still lacking. This work aims to address this by using a simple model of colloid-colloid interactions, incorporating both LJ-like and electrostatic interactions to characterise structures formed on a spherical droplet and investigate how these depend on the particle-particle interactions.

Inspired by recent experimental and simulation work [11] this paper will focus on binary mixtures of particles, examining conditions that give rise to mixed and demixed structures. The droplet is modelled as a stationary sphere. There is no explicit interaction between sphere and particles, rather the particles are constrained to move on the droplet surface. The colloidal particles interact through a combination of a LJ, to model short-range interactions, and Yukawa [22], accounting for screened electrostatic interactions:

$$E_{ij}(r_{ij}) = E_{ij}^{LJ}(r_{ij}) + E_{ij}^{Yukawa}(r_{ij}) = 4\varepsilon_{ij}\left[\left(\frac{\sigma_{ij}}{r_{ij}}\right)^{12} - \left(\frac{\sigma_{ij}}{r_{ij}}\right)^{6}\right] + A_{ij}\sigma_i^2\sigma_j^2\frac{\exp\left(-r_{ij}/\xi\right)}{r_{ij}/\xi} \quad (1)$$

where ε_{ij} is the well-depth, $\sigma_{ij} = (\sigma_i + \sigma_j)/2$ is the well width, A_{ij} is a prefactor related to the surface charge density on the colloidal particles, ξ is the screening length (here set to 1.00), and r_{ij} is the interparticle separation. For interactions between like-particles $\varepsilon_{ij} = 1.00$ and $A_{ij} = [0.00, 1.00]$, while for unlike particles $0.25 \leq \varepsilon_{ij} \leq 1$ and $A_{ij} = [-1.00, 1.00]$. The interactions cutoffs are set at $4\sigma_{ij}$. We set $k_B T^*/\varepsilon = 1$. All energies are in units of $k_B T^*$. Examples of the interparticle interactions are shown in Fig. 1; for positive A_{ij} this potential can exhibit a short range attractive well with a repulsive tail.

The system is studied using grand-canonical MC simulations [23]. At each simulation step a particle can be either moved, added, or removed. If the particle is moved, the new configuration will be accepted according to the Metropolis acceptance probability:

$$P(s \to s') = \min[1, e^{-\beta(E_{s'} - E_s)}] \quad (2)$$

where $E_{s'} - E_s$ is the difference in energy between the new configuration s' and the old configuration s and $\beta = \frac{1}{k_B T}$. Particle insertions and deletions are accepted according to

$$P(N \to N+1) = \min\left[1, \frac{1}{N+1} e^{\beta(\mu - E_{N+1} + E_N)}\right] \quad (3a)$$

$$P(N \to N-1) = \min\left[1, N e^{\beta(-\mu + E_N - E_{N-1})}\right] \quad (3b)$$

where μ is an effective chemical potential accounting also for the sphere-particle interactions and N the total number of particles in the system.

The choice of simulation parameters is motivated by recent experimental results [11]. The size ratio between large and small particles $r_2/r_1 = 1.67$ was chosen to correspond to the ratio of commercially available polystyrene spheres [11]. The droplet size was set to $R/r_1 = 6$, larger than in previous work to better study the self-assembled patterns. Simulations of both binary mixtures and single components systems were performed. We run simulations at $k_B T = 1.00, 0.75, 0.50, 0.40, 0.30, 0.20, 0.10$, using the last configuration of each temperature as starting configuration for the next, lower, temperature. At each temperature 200,000 MC sweeps were performed, where each sweep consisted on average of 500 attempted translations and 50 attempted insertions and deletions (120,000,000 attempted MC moves in total). All the simulations have been run in three replicas.

Binary mixtures exhibit a range of different structures, as shown in Fig. 2 for $k_B T = 0.10$. At $k_B T = 0.10$, corresponding to one tenth of the LJ interaction among like particles, we expect the patterns to be frozen. In the absence of electrostatic interactions (i.e. $A_{ij} = 0$) when the large particles greatly outnumber the small ones (i.e. with $N_b >> N_s$) the system typically forms a well ordered packing of the large particles with the small particles residing in the defects of this packing which, in turn, are surrounded by five large particles (Fig. 2a). For the opposite case, where $N_b << N_s$, the small particles similarly form a well-ordered packing. However, the defects in the small particle packing are too small for the large particles so disorder is seen over larger areas and a limited degree of aggregation between the large particles is found (Fig. 2b). When $N_b \sim N_s$ more complex patterns are observed, particularly when electrostatic interactions are considered. Oppositely charged particles with strong LJ-like interactions ($A_{ij} = -1.00$ and $\varepsilon_{ij} = 1.00$) form phases where both components are well mixed (Fig. 2c–d). Depending on

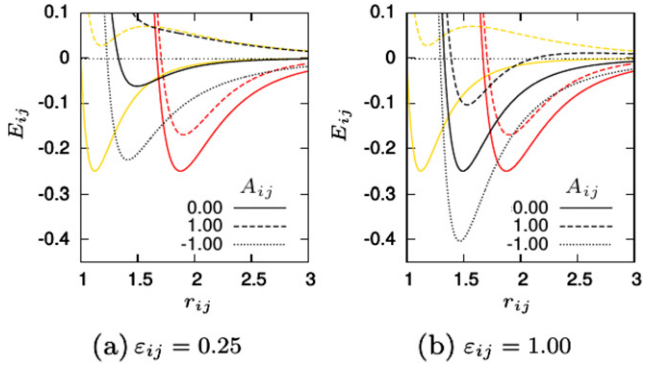

Fig. 1. Interparticle potentials between different sized particles (black line) at (a) $\varepsilon_{ij} = 0.25$ and (b) $\varepsilon_{ij} = 1.00$ for $A_{ij} = 0.00$ (solid), $A_{ij} = 1.00$ (dashed) and $A_{ij} = -1.00$ (dotted). For comparison, same sized interparticle potentials with $\varepsilon_{ij} = 1.00$ are shown for small (yellow) and large (red) particles.

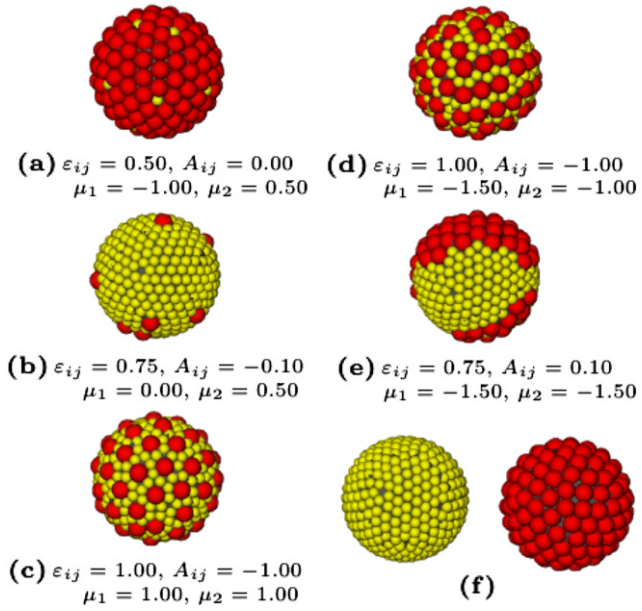

Fig. 2. Representative patterns formed at $k_B T = 0.10$. The patterns (a–f) are specific to selected values, while (f) has been found for all the explored μ at $\varepsilon_{ij} < 0.75$ and $A_{ij} > 0$.

the relative chemical potentials large particles are isolated from each other and surrounded by small particles ($\mu_1 = \mu_2 = 1.00$) or large and small particles form strings on the droplet surfaces ($\mu_1 = -1.50, \mu_2 = -1.00$). As well as mixed patterns, segregated (Fig. 2e) and single component packings (Fig. 2f) are found for like-charged particles with $A_{ij} > 0$ and $\varepsilon_{ij} \ll 1.00$.

By studying the packing patterns found for different combinations of the thermodynamic (μ_i) and potential parameters (A_{ij} and ε_{ij}) we can construct a low-temperature phase diagram (at $k_BT = 0.10$) as shown in Fig. 3. This two-dimensional projection on the A_{ij}-ε_{ij} plane can be used to illustrate how each packing is related to the potential parameters. For $\varepsilon_{ij} < 0.8$ and $A_{ij} > -0.2$ we find largely single component packings (Fig. S1a), with the identity of the particles on the droplet surface depending on their relative chemical potentials. In these cases the repulsive interactions between the unlike particles are too large to allow both components to reside on the surface.

At low values of ε_{ij} mixed packings can be formed for sufficiently negative A_{ij} where the electrostatic attraction can lead to mixing between the different components (Fig. S1d). Due to the strong attractive electrostatic interactions between unlike particles (and corresponding electrostatic repulsion between like particles) these correspond to packings where large and small particles are mixed together, such as isolated large particles and strings. Even in this region single-component patterns are found when μ_1 is much larger than μ_2. The same considerations apply for $\varepsilon_{ij} = 1.00$ and all values of A_{ij}. In this latter case mixed patterns become predominant when A_{ij} decreases.

Patterns consisting of segregated regions of large and small particles (as in Fig. S1b) are only observed for a narrow region between the single and two-component mixed packings. The narrow window of segregated phases can be understood as the repulsion between the unlike particles has to be large enough for the particles to demix from each other but not large enough to lead to single component packings. The transition can be observed by following the fraction of small and large particles at selected values of μ_1, μ_2 along ε_{ij} and A_{ij}. The trend can be appreciated for instance at $\mu_1 = -1.00$ and $\mu_2 = -0.50$, values for which the patterns observed are particularly sensitive to the choice of potential parameters.

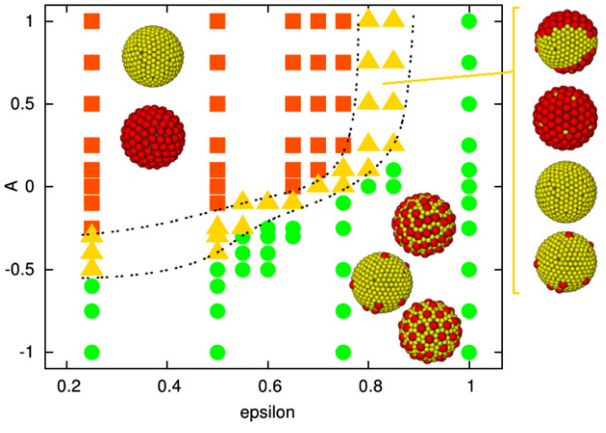

Fig. 3. Sketch diagram representing the 4-dimensional μ_1, μ_2, A_{ij},and ε_{ij} space. Each point of the diagram represents the possible end simulation configurations encountered at $k_BT = 0.10$ in the μ_1, μ_2 phase diagram calculated at the corresponding values of A_{ij}, ε_{ij}. Each point can represent the presence of only uniform coating of either particle (squares), both uniform coatings and segregation (triangles), either single coating or mixing (circles) found at at $k_BT = 0.10$ in μ_1, and μ_2 space. The dashed lines correspond to the boundaries between uniform coating, both uniform coatings and segregation, and single coating or mixing.

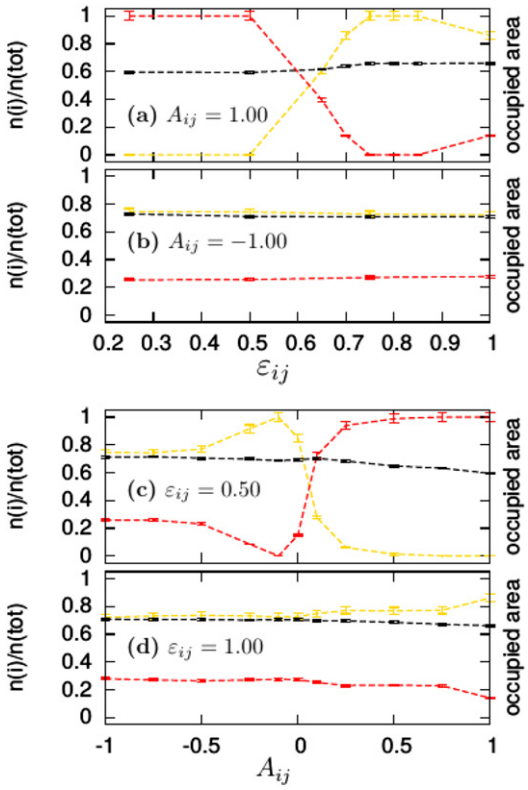

Fig. 4. Fraction of small (yellow) and large (red) particles and fraction of occupied surface (black) for constant values of A_{ij} (a,b) and ε_{ij} (b,c) at $\mu_1 = -1.00, \mu_2 = -0.50$.

In Fig. 4 we show how the packing patterns at at $k_BT = 0.10$ (where the surface is entirely covered by particles) are controlled through the potential parameters A_{ij} and ε_{ij}. For constant $A_{ij} = 1.00$ (Fig. 4a) the coverage, dominated by large particles at $\varepsilon_{ij} < 0.5$ become dominated by small ones for ε_{ij} approaching 1.00. In this case, at $\varepsilon_{ij} \simeq 0.6$ there is the crossover between the two populations, where the large particles appear as isolated defects on the surface. The fraction of small particles reaches a maximum at $\varepsilon_{ij} = 0.75$ and this is the region in which segregation can emerge. At values of ε_{ij} larger than 0.85 mixing occurs with a decrease in the fraction of small particles. This behaviour is not observed at $A_{ij} = -1.00$ (Fig. 4b) where the two particle populations are approximately constant along ε_{ij}, even if a large degree of order is observed in the patterns at $\varepsilon_{ij} = 1.00$, with the appearance of well mixed structures or stripes. Similar transitions are observed for the other values of the potential parameters, and also by following the process along A_{ij} at constant $\varepsilon_{ij} = 0.50$ (Fig. 4c), where segregation is observed for A_{ij} between -0.25 and -0.45. On the other hand, for $\varepsilon_{ij} = 1.00$ no crossover is observed and the fraction of small particles simply increases with A_{ij} (Fig. 4d).

These simulations demonstrate that through judicious choices of potential parameters the packing patterns of particles in spherical surfaces may be controlled. Experimentally such systems can be realised through the adsorption of colloidal nanoparticles onto fluid droplets, bilayer vesicles, or curved surfaces, or the formation of core-shell particles. This work demonstrates that the strength of the electrostatic interaction is a key parameter for controlling the formation of ordered patterns. While it is not always straightforward, the strength of interactions between colloidal particles can be controlled experimentally [24] through changing ionic strength, pH, or polymer concentration, giving a potential route for directing assembly of colloidal nanoparticles.

Supplementary data to this article can be found online at http://dx.doi.org/10.1016/j.colcom.2017.02.002.

Acknowledgements

We gratefully acknowledge the Academia Nazionale dei Lincei and the Royal Society of Edinburgh for the financial support. We thank the Scientific Computing Activity, IT Group, Sincrotrone Trieste SCpA for providing computing time on the THINK cluster, part of the Grid & Cloud Supercomputing Infrastructure.

References

[1] N. Vogel, M. Retsch, C.A. Fustin, A. Del campo, U. Jonas, Chem. Rev. 115 (13) (2015) 6265–6311.
[2] G.A. Ozin, S.M. Yang, Adv. Funtional Mater. 11 (2) (2001) 95–104.
[3] A. Stein, B.E. Wilson, S.G. Rudisill, Chem. Soc. Rev. 42 (7) (2013) 2763–2803.
[4] C. Fenzl, T. Hirsch, O.S. Wolfbeis, Angew. Chemie - Int. Ed. 53 (13) (2014) 3318–3335.
[5] E. Kumacheva, R.K. Golding, M. Allard, E.H. Sargent, Adv, Mater. 14 (3) (2002) 221–224.
[6] F. Zaera, Chem. Soc. Rev. 42 (7) (2013) 2746–2762.
[7] F. Caruso, Adv.Mater. 13 (1) (2001) 11–22.
[8] M. Motornov, Y. Roiter, I. Tokarev, S. Minko, Prog. Polym. Sci. 35 (12) (2010) 174–211.
[9] E. Duguet, A. Désert, A. Perro, S. Ravaine, Chem. Soc. Rev. 40 (2) (2011) 941–960.
[10] J. Zhu, A. Tang, L.P. Law, M. Feng, K.M. Ho, D.K.L. Lee, F.W. Harris, P. Li, Bioconjug. Chem. 16 (1) (2005) 139–146.
[11] R. Chen, D.J.G. Pearce, S. Fortuna, D.L. Cheung, S.A.F. Bon, Amer. Chem. Soc. 133 (7) (2011) 2151–2153.
[12] S. Fortuna, C.A.L. Colard, A. Troisi, S.A.F. Bon, Langmuir 25 (21) (2009) 12399–12403. (b) Gaulding, J. C.; Saxena, S.; Montanari, D. E.; Lyon, L. A. ACS Macro Letters 2013, 2(4) 337-340.
[13] A. Walther, A.H.E. Mueller JANUS PARTICLE SYNTHESIS, SELF-ASSEMBLY AND APPLICATIONS, Jiang, S and Granick, S., number 1 in RSC Smart Materials, ROYAL SOC CHEMISTRY England, 2012 1–28. (b) Walther, A.; Müller, A. H. E. Chem. Rev. 2013, 113(7), 5194-5261.
[14] S.C. Glotzer, M.J. Solomon, Nature Materials 6 (8) (2007) 557–562.
[15] N.A. García, A.D. Pezzutti, R.A. Register, D.A. Vega, L.R. Gómez, Soft Matter 11 (5) (2015) 898–907.
[16] S. Paquay, R. Kusters, Biophys J. 110 (6) (2016) 1226–1233.
[17] S. Paquay, H. Kusumaatmaja, D.J. Wales, R. Zandi, P. van der Schoot, Soft Matter 12 (2016) 1–25.
[18] A. Dinsmore, M.F. Hsu, M. Nikolaides, M. Marquez, A. Bausch, D. Weitz, Science 298 (5595) (2002) 1006–1009. (b) Lipowsky, P.; Bowick, M. J.; Meinke, J. H.; Nelson, D. R.; Bausch, A. R. Nat. Mater. 2005, 4(May), 407-411. (c) Bowick, M. J.; Nelson, D. R.; Travesset, A. Phys. Rev. B 2000, 62, 8738-8751. (d) Jiménez, F. L.; Stoop, N.; Lagrange, R.; Dunkel, J.; Reis, P. M. Phys. Rev. Lett. 2016, 116, 104301.
[19] C. Singh, P.K. Ghorai, M.A. Horsch, A.M. Jackson, R.G. Larson, F. Stellacci, S.C. Glotzer, Phys, Rev. Lett. 99 (2007) 226106. (b) Ghorai, P. K.; Glotzer, S. C. J. Phys.Chem.C 2010 114(45) 19182-19187.
[20] F. Sciortino, A. Giacometti, G. Pastore, Phys. Rev. Lett, 103 (2009) 237801. (b) Bott, M. C.; Brader, J. M. Phys. Rev. E 2016, 94(1), 012603.
[21] J.A. Balmer, O.O. Mykhaylyk, A. Schmid, S.P. Armes, J.P.A. Fairclough, A.J. Ryan, Langmuir 27 (13) (2011) 8075–8089.
[22] H. Yukawa, Nippon Sugaku-Buturigakkwai Kizi Dai 3 Ki 17 (0) (1935) 48–57.
[23] D. Frenkel, B. Smit, Understanding molecular simulation. From algorithms to applications; Academic Press: San Diego 2nd ed., 2002.
[24] A. Yethiraj, Soft Matter 3 (9) (2007) 1099.